ACADEMIC PRESS

Journal of Solid State Chemistry 169 (2002) 85–95

JOURNAL OF SOLID STATE CHEMISTRY

www.academicpress.com

Evolution of magnetic state in the $La_{1-x}Ca_xMnO_{3-\gamma}$ ($x = 0.30, 0.50$) manganites depending on the oxygen content

S.V. Trukhanov,[a,*] N.V. Kasper,[a,b] I.O. Troyanchuk,[a] M. Tovar,[c] H. Szymczak,[d] and K. Bärner[e]

[a] *Belarus Institute of Solids and Semiconductor Physics, National Academy of Sciences, P. Brovka str. 17, 220072 Minsk, Russia*
[b] *Max-Planck-Institut für Metallforschung, Heisenberg str.1, D-70569 Stuttgart, Germany*
[c] *Hahn-Meitner-Institute (BENSC), Glienicker str. 100, D-14109 Berlin, Germany*
[d] *Institute of Physics, PAS, Lotnikov str. 32/46, 02-668 Warsaw, Poland*
[e] *IY. Physikalisches Institut der Universität Göttingen, Bunsenstrasse 13-15, D37073 Göttingen, Germany*

Received 18 April 2002; received in revised form 11 July 2002; accepted 27 August 2002

Abstract

The crystal structure, magnetic and electrical properties of the $La_{1-x}Ca_xMnO_{3-\gamma}$ ($x = 0.30$, 0.50; $0 \leqslant \gamma \leqslant 0.50$) oxygen-deficient manganites have been studied. It is found that the compounds $La_{0.70}Ca_{0.30}MnO_{3-\gamma}$ possess a long-range ferromagnetic order up to $\gamma = 0.06$ and a cluster spin glass behavior at $0.06 < \gamma \leqslant 0.20$. Antiferromagnetic state of $La_{0.50}Ca_{0.50}MnO_{3-\gamma}$ ($\gamma = 0$) composition transforms into inhomogeneous ferromagnetic one at $\gamma = 0.04$. The system converts into cluster spin glass state at $\gamma = 0.10$. As oxygen deficit reaches the value $\gamma = 0.25$, a new type of ferromagnetic phase appears. The fraction of this ferromagnetic phase is the highest in the composition $\gamma = 0.30$. It is supposed that the compounds with $\gamma \geqslant 0.35$ represent an antiferromagnetic medium with inclusions of the ferromagnetic phase. The strongly reduced samples exhibit a large magnetoresistance below the temperature, at which the spontaneous magnetization develops. The magnetic phase diagrams of both $La_{0.70}Ca_{0.30}MnO_{3-\gamma}$ and $La_{0.50}Ca_{0.50}MnO_{3-\gamma}$ systems have been constructed. We argue, that the oxygen vacancies are disordered in the $La_{0.70}Ca_{0.30}MnO_{3-\gamma}$ system in the studied region of oxygen vacancies concentration ($0 \leqslant \gamma < 0.20$) whereas for the $La_{0.50}Ca_{0.50}MnO_{3-\gamma}$ they tend to order at $\gamma > 0.25$ in a manner of $Sr_2Fe_2O_5$-type crystal structure. This study shows that Mn^{3+}–O–Mn^{3+} ferromagnetic interaction may play an important role in the formation of magnetic state of manganites.

PACS: 75.30.Kz; 75.30.Vn; 75.50.Dd

Keywords: Manganite; Oxygen deficit; Cluster spin glass; Magnetoresistance; Magnetic state

1. Introduction

The discovery of such collective electronic phenomena as a colossal magnetoresistance, metal–insulator and charge order–disorder phase transitions induced by external magnetic field renewed the interest in compounds of the $Ln_{1-x}A_xMnO_3$ (Ln = trivalent rare-earth elements from Pr^{3+} to Tb^{3+} and La^{3+}; A = divalent elements such as Ca^{2+}, Sr^{2+}, Ba^{2+}, Cd^{2+}, Pb^{2+}) systems [1,2]. Astonishing magnetic and electrical properties of these hole-doped manganites become a subject of numerous experimental [3,4] and theoretical [5,6] investigations. Reasons for this interest are the various linkages of the properties of metals and insulators, ionic and covalent crystals with intermediate ion valence, systems with spin, orbital and charge ordering and, lastly, systems which can undergo a phase separation. These properties result from a close interplay of lattice, charge and spin degree of freedom that gives rise to complex phase diagrams for these classes of compounds [7,8].

At present, $La^{3+}_{1-x}Ca^{2+}_x Mn^{3+}_{1-x}Mn^{4+}_x O^{2-}_3$ system is the most investigated. The parent $LaMnO_3$ compound is A-type antiferromagnetic insulator with a small

*Corresponding author. Fax: +7-375-172-84-0888.
E-mail addresses: truhanov@ifttp.bas-net.by (S.V. Trukhanov), kasper@ifttp.bas-net.by (N.V. Kasper).

0022-4596/02/$ - see front matter © 2002 Elsevier Science (USA). All rights reserved.
PII: S0022-4596(02)00028-2

ferromagnetic component due to the non-collinearity of the manganese magnetic moments, i.e., weak ferromagnet. An orbital ordering is observed in $LaMnO_3$ and the SE magnetic interaction of manganese ions is anisotropic as a result of the Jahn–Teller effect.

Substitution of La^{3+} by Ca^{2+} ions enhances an average manganese valence to conserve the whole electrical neutrality and formally produces Mn^{4+} ions with t_{2g}^3 ($S = 3/2$) electronic configuration. In this case, e_g electrons of Mn^{3+} are assumed to be delocalized and play a role as charge carriers. This system exhibits insulator–metal concentration phase transitions at $0.15 < x < 0.50$ as well as antiferromagnet–ferromagnet one [9]. The ferromagnetic and metallic properties for $La_{1-x}Ca_xMnO_3$ system almost simultaneously appear. However, till now there is no complete clarity whether these properties assist one another or not.

There are two peculiar x values for $La_{1-x}Ca_xMnO_3$. Most of the recent researches on these materials are focused on compounds with $x = 0.30$ displaying a large magnetoresistance ($\sim 10^8$% [10]) associated with a first-order phase transition into ferromagnetic conducting ground state from the paramagnetic insulating one near T_C [11]. Another critical doping level is $x = 0.50$. In contrast to $x = 0.30$, the magnetoresistance for this point is associated with a first-order antiferromagnet–ferromagnet and field-induced insulator–metal phase transitions.

In particular, we can recall that $La_{0.70}Ca_{0.30}MnO_3$ compound is a paramagnetic semiconductor above $T_C \approx 272$ K and becomes a ferromagnetic metal at cooling while $La_{0.50}Ca_{0.50}MnO_3$ is a paramagnetic semiconductor above $T_C \approx 260$ K and a charge-ordered antiferromagnetic (CE-type) semiconductor below $T_N \approx 180$ K (on warming). Between T_C and T_N, $La_{0.50}Ca_{0.50}MnO_3$ consists of hole-poor ferromagnetic metallic clusters embedded in a paramagnetic charge-ordered matrix [12, 13]. Thus, $La_{0.50}Ca_{0.50}MnO_3$ is an insulator at the entire temperature range. The CE-type magnetic order is characterized by the ordering of Mn^{3+} and Mn^{4+} moments alternately. The spin ordering in the *ab* plane is somewhat complex and it becomes antiferromagnetic along the *c*-axis [14]. It is notable that the long-range charge and antiferromagnetic ordering in $La_{0.50}Ca_{0.50}MnO_3$ are established simultaneously ($T_N = T_{CO}$). However, short-range charge ordering starts to develop around 210 K, well above the ferromagnetic–antiferromagnetic phase transition [15]. In the charge-ordered state e_g electrons are localized in the crystal lattice creating a periodical ordering of Mn^{3+} and Mn^{4+} ions [16].

It is believed that the double exchange (DE) interaction between Mn^{3+} and Mn^{4+} pairs controls magnetic and electrical properties of perovskite manganites [17,18]. This model is based on the real exchange of e_g electrons between two partially filled *d* shells of Mn^{3+} and Mn^{4+} ions. However, DE alone cannot explain all the existing facts [19,20]. Goodenough [21] suggested that ferromagnetism is not governed by DE alone but also by the specific nature of the superexchange interactions (SE) in the Mn^{3+}–O–Mn^{3+} and Mn^{3+}–O–Mn^{4+} Jahn–Teller ion systems. He proposed that in the case when the static Jahn–Teller distortions are removed, the orbital configuration of the 3*d* electrons is determined by the position of the ion nuclei (Goodenough's quasistatic hypothesis). In the SE model, the ferromagnetic fraction of the exchange is determined by a virtual electron transfer from the half-filled e_g orbitals of the Mn^{3+} ions to the empty ones.

By changing the Mn^{3+}/Mn^{4+} ratio one may modify the contribution from the DE and SE interactions; therefore, it is interesting to investigate $La_{1-x}Ca_xMnO_{3-\gamma}$ compounds depending on the formal average manganese valence. The Mn^{i+}/Mn^{j+} (where i, $j = 2, 3, 4$) ratio can be changed by various methods [22]. Until now the dependence of magnetic and magnetoresistance properties of the hole-doped perovskite manganites on oxygen stoichiometry has not been investigated sufficiently deeply. The removal of oxygen ions from the $Ln_{1-x}^{3+}A_x^{2+}Mn_{1-x+2\gamma}^{3+}Mn_{x-2\gamma}^{4+}O_{3-\gamma}^{2-}$ produces a reduction process when Mn^{4+} ions are converted to Mn^{3+} and their coordination number decreases. The reduction of the manganites usually enhances the resistivity value and suppresses both the spontaneous magnetization and the Curie temperature. It has been confirmed that the oxygen deficiency and the ordering of the oxygen vacancies are closely related to the cationic ordering in the perovskite lattice [23].

However, very intriguing magnetic and magnetoresistance properties have been recently revealed for $La_{1-x}Ca_xMnO_{3-\gamma}$ [24,25] and $Pr_{1-x}Ba_xMnO_{3-\gamma}$ [26] compounds with oxygen vacancies. The obtained results have shown the unconventional features for these strongly reduced manganites such as: large ferromagnetic component and magnetic ordering temperature as well as large magnetoresistance in spite of the absence of Mn^{3+}–Mn^{4+} pairs. The oxygen vacancies are supposed to be ordered.

Taking the above-mentioned into account we report in this paper that the magnetization, electrical resistivity and magnetoresistance properties of $La_{1-x}Ca_xMnO_{3-\gamma}$ ($0 \leqslant \gamma \leqslant 0.50$) reduced manganites for two selected doping levels: $x = 0.30$, 0.50. Our investigations have allowed to construct hypothetical magnetic phase diagrams.

2. Experiment

Polycrystalline $La_{1-x}Ca_xMnO_3$ ($x = 0.30$; 0.50) samples have been fabricated with conventional ceramic

technology. La_2O_3 (99.99%), $CaCO_3$ (99.99%) and MnO_2 (99.99%) have been mixed in designed cation ratios (La:Ca:Mn = [1−x]:x 1) and ground in an agate mortar with a small value of ethanol. Since the La_2O_3 powder tends to adsorb CO_2 and H_2O contained in air, the La_2O_3 oxide has been dried at 1000°C for 2 h before weighing. The obtained mixtures have been pressed into pellets and prefired at 1100°C for 2 h in air to decompose calcium carbonate to calcium oxide. The obtained pellets were again ground, compacted and synthesized at 1550°C during 2 h in air followed by slow cooling at a rate of 80°C/h in order to obtain the stoichiometric oxygen content. All the synthesized compounds have been checked by powder X-ray diffraction method to determine the qualitative phase content and unit-cell parameters. X-ray data have been recorded at room temperature with a DRON-3 diffractometer in Cr$K\alpha$ radiation in the range $30^\circ \leqslant 2\theta \leqslant 100^\circ$. Neutron diffraction measurements for $La_{0.50}Ca_{0.50}MnO_{2.50}$ sample have been performed in the Berlin Neutron Scattering Center using the E9 neutron powder diffractometer (FIREPOD) with a wavelength of neutrons $\lambda = 1.79686$ Å and scanning step $\Delta\theta \sim 0.002^\circ$. A sapphire single-crystal filter of total thickness of 110 mm in the primary beam was used to reduce the number of epithermal neutrons. In order to increase the neutron flux at the sample a vertically focusing Riso-design Ge-monochromator was used. The oxygen content of all the sintered samples has been determined by thermogravimetric analysis (TGA). These investigations have shown the oxygen content to be almost stoichiometric. As it is known the deviation of the oxygen stoichiometry for the manganites prepared by the aforementioned technique was negligible [7]. We determined the Mn valence by redox titration. This study gave values of Mn^{4+} concentration equal to 30% and 49% for the stoichiometric $La_{0.70}Ca_{0.30}MnO_3$ and $La_{0.50}Ca_{0.50}MnO_3$ compounds, respectively. The differences between the contents of Mn^{4+} and x appear probably from small oxygen non-stoichiometry or cation impurities.

Polycrystalline-reduced samples $La_{0.70}Ca_{0.30}MnO_{3-\gamma}$ ($\gamma = 0$, 0.06, 0.08, 0.11, 0.15, 0.20) and $La_{0.50}Ca_{0.50}MnO_{3-\gamma}$ ($\gamma = 0.01$; 0.04; 0.10; 0.12; 0.17; 0.20; 0.22; 0.25; 0.27; 0.30; 0.31; 0.32; 0.35; 0.37; 0.45; 0.48; 0.50) were obtained by the topotactic reaction method. The topotactic reaction is one without considerable changes of the as-prepared sample structure. The crystal lattice of the topotactic reaction product depends on the existing structural elements in the starting material. Often the topotactic product is metastable. To obtain the oxygen vacancies, the samples have been treated in the evacuated silica tubes at 900°C during 2 h using metallic tantalum as an oxygen producer. This reduction may be described by the equation

$$La_{1-x}Ca_xMnO_3 + (2\gamma/5)Ta \rightarrow La_{1-x}Ca_xMnO_{3-\gamma} + (\gamma/5)Ta_2O_5. \quad (1)$$

The final oxygen content was calculated from a change of the sample weight after reduction. About 2–3 g of the sample is usually placed into a tube. Relative error of the oxygen content measurements did not exceed 0.3%. To check the oxygen content in the reduced samples they were subjected to reoxidation in air at 900°C during 2 h. The weight gain resulted from reoxidation indicated that the oxygen-deficit γ of the reduced samples was found with an error of ± 0.01. This fact confirms the topotactic character of the reduction because an important feature of the oxygen-deficient perovskite compounds is their ease of reoxidation with the restoration of their initial composition, structure and physical properties.

The magnetization measurements were made using a MPMS-7 Quantum Design SQUID magnetometer and OI-3001 commercial vibrating sample magnetometer in the temperature range 4–300 K. The magnetic transition temperature was defined as an intersection point of the tangent to the magnetization curve at maximum slope with temperature axis. The electrical resistivity was been obtained by a standard four-probe method in the temperature range 77–300 K. Indium eutectic was been employed for ultrasonic deposition of contacts. For these measurements, well-sintered samples in the form of parallelepiped with $10 \times 2 \times 2\,mm^3$ dimensions were used. The magnetoresistance was calculated according to the relation

$$MR = \{[\rho(H) - \rho(H=0)]/\rho(H=0)\}100\%, \quad (2)$$

where MR is the magnetoresistance, $\rho(H)$ is the resistivity in magnetic field of 9 kOe, and $\rho(H=0)$ is the resistivity without magnetic field. Applied magnetic field was applied parallel to the current in the sample during magnetoresistance measurements.

3. Results and discussion

According to X-ray measurements, the $La_{1-x}Ca_xMnO_3$ as-prepared samples with $x = 0.30$ and 0.50 compositions were nominally single-phase perovskites with O-orthorhombic unit cell ($a < c/\sqrt{2} < b$). X-ray data for the $La_{1-x}Ca_xMnO_{3-\gamma}$-reduced series of the samples are more complex. All the reduced samples with $x = 0.30$ as well as $x = 0.50$, $\gamma \leqslant 0.25$ retained the O-orthorhombic perovskite structure. The $x = 0.50$ samples with $\gamma > 0.25$ were diphasic with a perovskite structure of $La_{0.50}Ca_{0.50}MnO_{3-\lambda}$ ($0 \leqslant \lambda \leqslant 0.50$) and $(La_{0.50}Ca_{0.50})_2Mn_2O_5$ similar to $Sr_2Fe_2O_5$ [27]. The latter type of structure is characterized with alternate [MnO_6] octahedral- and [MnO_4] tetrahedral-like oxygen

coordination of manganese ions. The structure of $Sr_2Fe_2O_5$ differs from that of the brownmillerite-type $Ca_2Fe_2O_5$, though both these structures are derived by the strong reduction of perovskite-type structure with the oxygen vacancies ordered along alternate rows [28].

As it is well known from the thermodynamics, a two-phase coexisting region should appear with decreasing oxygen content below some critical value when oxygen vacancies ordering occurs. This possibility may be realized in the case of $x = 0.50$ when γ rises above 0.25. We believe that at the $\gamma \geqslant 0.25$, the crystal structure transition takes place and compounds from the range $(0.25 \leqslant \gamma \leqslant 0.50)$ present mixture with respect to crystal structure from the $(La_{0.50}Ca_{0.50})_2Mn_2O_5$ phase with highest possible oxygen vacancies $\gamma = 0.50$ and $La_{0.50}Ca_{0.50}MnO_{3-\lambda}$, the one with oxygen vacancies value λ continuously increases from 0 to 0.50. So, total oxygen vacancies concentration γ is determined as $0.50n_1 + \lambda n_2$, where n_1 and n_2 are the volume fractions of first and second phases, respectively. The free energy depending on the oxygen vacancies concentration curves are different for $La_{0.50}Ca_{0.50}MnO_{2.75}$ and $(La_{0.50}Ca_{0.50})_2Mn_2O_5$. The free energy minimum requires coexistence of a two-phase state. The two-phase region is also observed for $LaMnO_{3+\delta}$ at the transformation from a orthorhombic to a rhombohedral structure (at $0.06 \leqslant \delta \leqslant 0.10$) as δ increases [29,30]. Thus, we suppose that as the γ value rises above 0.25 the crystal structure of the $La_{0.50}Ca_{0.50}MnO_{3-\gamma}$ undergoes a phase separation into an $(La_{0.50}Ca_{0.50})_2Mn_2O_5$ phase and that with some higher oxygen content than nominal one. This separation goes in such a manner that the total oxygen content of two phases corresponds to a nominal γ value.

The unit-cell parameters are collected in Tables 1 and 2. For the compounds $La_{0.50}Ca_{0.50}MnO_{3-\gamma}$ with $\gamma > 0.25$, we were unable to identify and divide clearly the crystal structure phases. So parameters for these samples are generally concerned with $(La_{0.50}Ca_{0.50})_2Mn_2O_5$ phase. The volume of the unit cell for all the reduced samples monotonically increases with γ. The increase of the volume is supposed to be due to the conversion of Mn^{4+} ions into Mn^{3+}. The effective ionic radii of Mn^{3+} and Mn^{4+} in octahedral oxygen coordination are 0.645 and 0.530 Å, respectively [31].

Table 1
Crystal structure parameters (a, b, c and V) for the samples of the $La_{0.70}Ca_{0.30}MnO_{3-\gamma}$ $(0 \leqslant \gamma \leqslant 0.20)$ reduced series

Composition	a (Å)	b (Å)	c (Å)	V (Å^3)
$La_{0.70}Ca_{0.30}MnO_3$	5.426	5.545	7.712	232.03
$La_{0.70}Ca_{0.30}MnO_{2.94}$	5.442	5.542	7.728	233.07
$La_{0.70}Ca_{0.30}MnO_{2.92}$	5.448	5.541	7.731	233.38
$La_{0.70}Ca_{0.30}MnO_{2.89}$	5.456	5.539	7.739	233.88
$La_{0.70}Ca_{0.30}MnO_{2.85}$	5.473	5.536	7.758	235.06
$La_{0.70}Ca_{0.30}MnO_{2.80}$	5.490	5.534	7.774	236.19

Table 2
Crystal structure parameters (a, b, c and V) for the samples of the $La_{0.50}Ca_{0.50}MnO_{3-\gamma}$ $(0 \leqslant \gamma \leqslant 0.50)$ reduced series

Composition	a (Å)	b (Å)	c (Å)	V (Å^3)
$La_{0.50}Ca_{0.50}MnO_3$	5.396	5.440	7.651	224.59
$La_{0.50}Ca_{0.50}MnO_{2.99}$	5.396	5.442	7.654	224.71
$La_{0.50}Ca_{0.50}MnO_{2.96}$	5.401	5.447	7.658	225.29
$La_{0.50}Ca_{0.50}MnO_{2.88}$	5.415	5.461	7.678	227.04
$La_{0.50}Ca_{0.50}MnO_{2.83}$	5.424	5.472	7.688	228.17
$La_{0.50}Ca_{0.50}MnO_{2.80}$	5.429	5.476	7.696	228.80
$La_{0.50}Ca_{0.50}MnO_{2.75}$	5.436	5.485	7.706	229.77
$La_{0.50}Ca_{0.50}MnO_{2.70}$	5.141	17.475	5.136	461.38
$La_{0.50}Ca_{0.50}MnO_{2.69}$	5.145	17.478	5.140	462.21
$La_{0.50}Ca_{0.50}MnO_{2.68}$	5.147	17.480	5.143	462.71
$La_{0.50}Ca_{0.50}MnO_{2.65}$	5.153	17.483	5.149	463.87
$La_{0.50}Ca_{0.50}MnO_{2.63}$	5.157	17.488	5.153	464.73
$La_{0.50}Ca_{0.50}MnO_{2.55}$	5.175	17.491	5.171	468.06
$La_{0.50}Ca_{0.50}MnO_{2.52}$	5.181	17.498	5.179	469.42
$La_{0.50}Ca_{0.50}MnO_{2.50}$	5.185	17.501	5.184	470.32

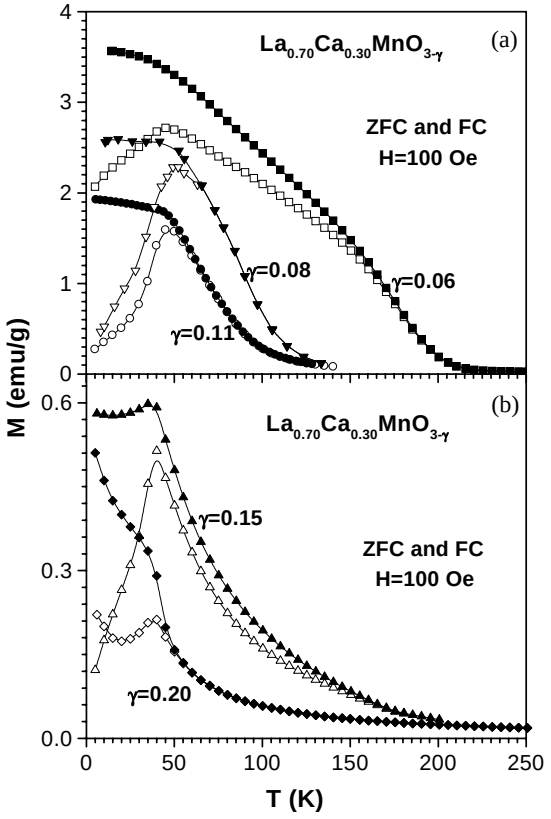

Fig. 1. The ZFC (open symbols) and FC (full symbols) magnetizations versus temperature curves in field of 100 Oe for the $La_{0.70}Ca_{0.30}MnO_{3-\gamma}$ reduced samples with $\gamma = 0.06$ (square), 0.08 (down-triangle), 0.11 (circle) (a) and 0.15 (up-triangle), 0.20 (diamond) (b).

The oxygen vacancies should reduce the unit-cell volume, whereas the transformation of Mn^{4+} into Mn^{3+} must give rise to it. Our data indicate that the last process dominates.

Fig. 1 displays zero-field-cooled (ZFC) and field-cooled (FC) magnetizations versus temperature in a

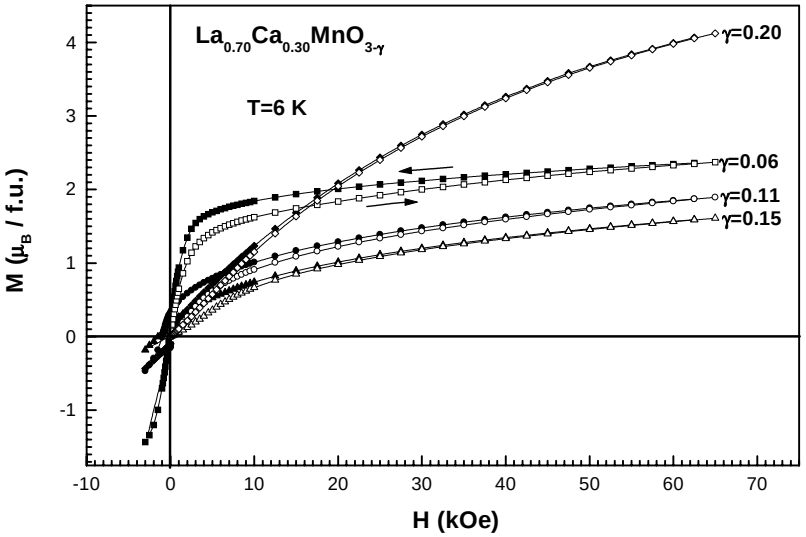

Fig. 2. The magnetization versus magnetic field curves at $T = 6\,\mathrm{K}$ for the $La_{0.70}Ca_{0.30}MnO_{3-\gamma}$ reduced samples with $\gamma = 0.06$ (square), 0.11 (circle), 0.15 (up-triangle) and 0.20 (diamond). Open symbols denote magnetization values at the increase of the field, full symbols—at the decrease.

field of 100 Oe for the $La_{0.70}Ca_{0.30}MnO_{3-\gamma}$-reduced samples. It is seen that the magnetic ordering temperature (T_{MO}) decreases with increasing number of the oxygen vacancies. The parent $La_{0.70}Ca_{0.30}MnO_3$ compound is ferromagnetically ordered up to $T_C = 250\,\mathrm{K}$ whereas the $\gamma = 0.06$ sample shows the Curie point slightly below 200 K. ZFC magnetization of the samples in the range $0.08 \leqslant \gamma \leqslant 0.20$ shows a peak, typical for the cluster spin glasses. It is notable that the temperature of this peak is almost constant in this oxygen vacancies range. The transition to the paramagnetic state is relatively broad. The sample with $\gamma = 0.20$ display a the sharp rise of the FC magnetization around 40 K where ZFC curve exhibits a peak.

Magnetization versus field dependences for $La_{0.70}Ca_{0.30}MnO_{3-\gamma}$ samples ($\gamma = 0.06$, 0.11, 0.15, 0.20) at $T = 6\,\mathrm{K}$ are presented in Fig. 2. The spontaneous magnetization (M_S) drops from $\sim 3.5\,\mu_B$/f.u. ($\gamma = 0$) down to $M_S \approx 1.75\,\mu_B$/f.u. for the $\gamma = 0.06$ sample. The value calculated for the pure ferromagnetic state is $3.70\,\mu_B$/f.u assuming $\mu(Mn^{3+}) = 4\,\mu_B$ and $\mu(Mn^{4+}) = 3\,\mu_B$. Magnetization of the $\gamma = 0.06$ sample shows a noticeable field hysteresis up to 50 kOe. M_S decreases with increasing number of the oxygen vacancies. The surprise is that the strongly reduced $\gamma = 0.20$ sample has a larger high-field magnetic susceptibility than other reduced samples. It is impossible to determine M_S for the $\gamma > 0.06$ samples because the magnetization is not saturated in the available fields up to 70 kOe. Magnetization for the $\gamma = 0.20$ sample is around $4\,\mu_B$/f.u. at field of 60 kOe.

Resistivity and magnetoresistance against temperature for the $\gamma = 0.06$, 0.11, 0.15, 0.20 samples of the $La_{0.70}Ca_{0.30}MnO_{3-\gamma}$ series are shown in Fig. 3. The $\gamma = 0.06$ sample gradually undergoes the metal–insulator

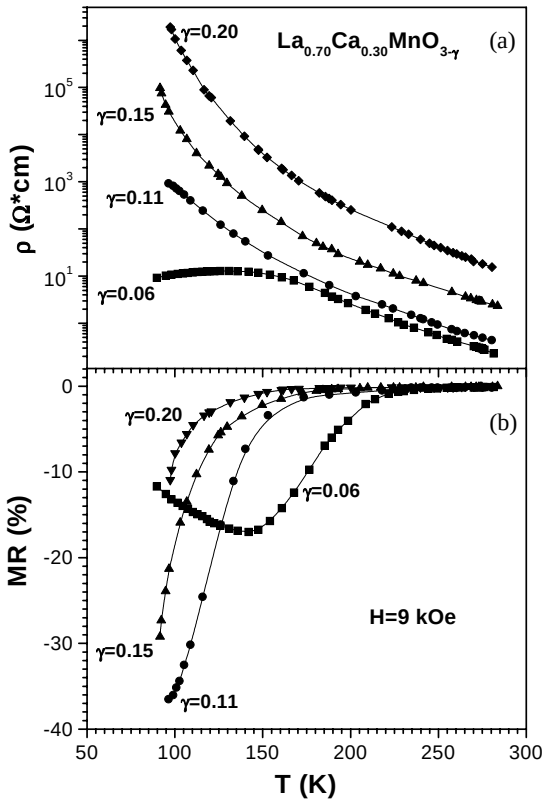

Fig. 3. The resistivity (a) and magnetoresistance (b) versus temperature curves for the $\gamma = 0.06$ (square), 0.11 (circle), 0.15 (up-triangle) and 0.20 (diamond) samples of the $La_{0.70}Ca_{0.30}MnO_{3-\gamma}$ reduced series.

transition starting from 150 K which is well below the Curie point $T_C \approx 200\,\mathrm{K}$. Resistivity of the samples with $\gamma \geqslant 0.08$ shows an insulating behavior and continuously increases as oxygen content decreases. Magnetoresistance displays non-monotonic evolution with γ. The

magnetoresistance for the $\gamma = 0.06$ sample has a peak at $\sim 18\%$ slightly below 150 K. Magnetoresistance of all the other samples appears nearly the magnetic ordering temperature and continuously increases on cooling down to liquid nitrogen temperature. The maximal value of MR $\sim 38\%$ has been observed in the sample $\gamma = 0.11$.

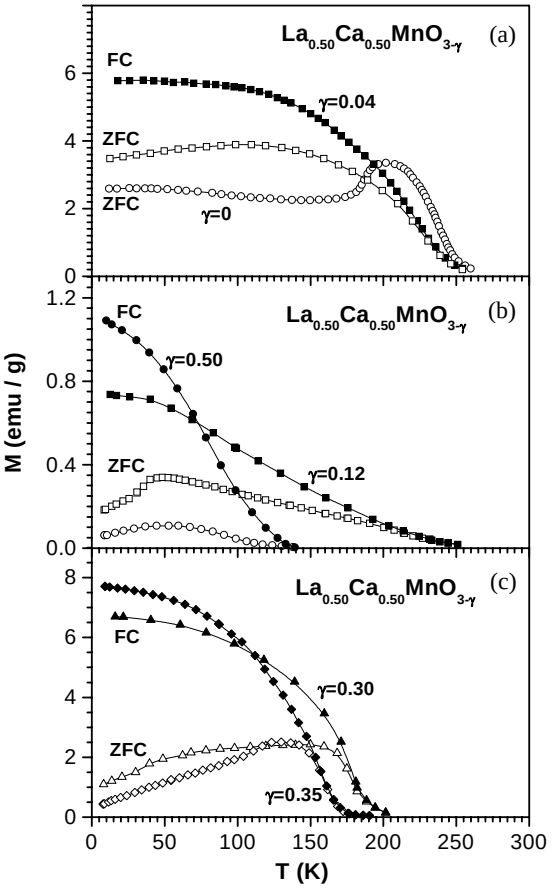

Fig. 4. The ZFC (open symbols) and FC (full symbols) magnetizations versus temperature curves in field of 100 Oe for the $La_{0.50}Ca_{0.50}MnO_{3-\gamma}$ reduced samples with $\gamma = 0$ (circle) and 0.04 (square) (a), $\gamma = 0.12$ (square), 0.50 (circle) (b) and 0.30 (up-triangle), 0.35 (diamond) (c).

Fig. 4 displays the ZFC and FC magnetizations versus temperature in a field of 100 Oe for the selected reduced samples of the $La_{0.50}Ca_{0.50}MnO_{3-\gamma}$ series. It is shown that T_{MO} monotonically decreases with increasing oxygen deficit. Removal of the oxygen ions challenges antiferromagnet–ferromagnet transition for $\gamma = 0.04$. ZFC magnetization shows a strong rise with increasing temperature up to ~ 50 K in the concentration range $0.12 \leqslant \gamma \leqslant 0.25$ whereas for $0.25 \leqslant \gamma \leqslant 0.50$ this effect is much less pronounced. The transition to the paramagnetic state occurs in a wide temperature range.

Magnetization versus the field curves for the selected reduced samples of the $La_{0.50}Ca_{0.50}MnO_{3-\gamma}$ series is presented in Fig. 5. For the $\gamma = 0.04$ sample the M_S value is 2.65 μ_B/f.u., which is below the calculated value for the pure ferromagnetic state (3.52 μ_B/f.u.). M_S decreases with oxygen content up to $\gamma = 0.20$. In the range $0.12 \leqslant \gamma \leqslant 0.20$, spontaneous magnetization does not exceed 0.2 μ_B/f.u. The surprise is that the spontaneous magnetization shows a maximum at the content of oxygen vacancies equal to 0.30. However, magnetic moment at 6 K is only around 1.5 μ_B per manganese ion whereas for the truly ferromagnetically ordered phase the expected value is 4.1 μ_B/f.u.

For the sample $\gamma = 0.50$ the spontaneous magnetization develops below 120 K. The spontaneous magnetic moment at $T = 5$ K does not exceed 0.2 μ_B per manganese ion. In order to establish the ground magnetic state of the $\gamma = 0.50$, sample the neutron diffraction measurements were performed. We have observed a few additional magnetic peaks which start to grow at temperature below 120 K (Fig. 6). Our preliminary analysis is in agreement with complex

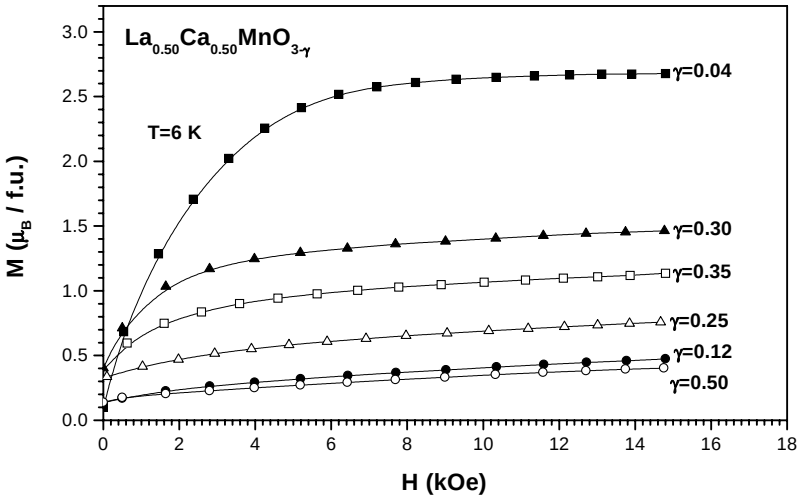

Fig. 5. The magnetization versus magnetic field curves at $T = 6$ K for the $\gamma = 0.04$ (full square), 0.12 (full circle), 0.30 (full up-triangle), 0.35 (open square) and 0.50 (open circle) samples of the $La_{0.50}Ca_{0.50}MnO_{3-\gamma}$ reduced series.

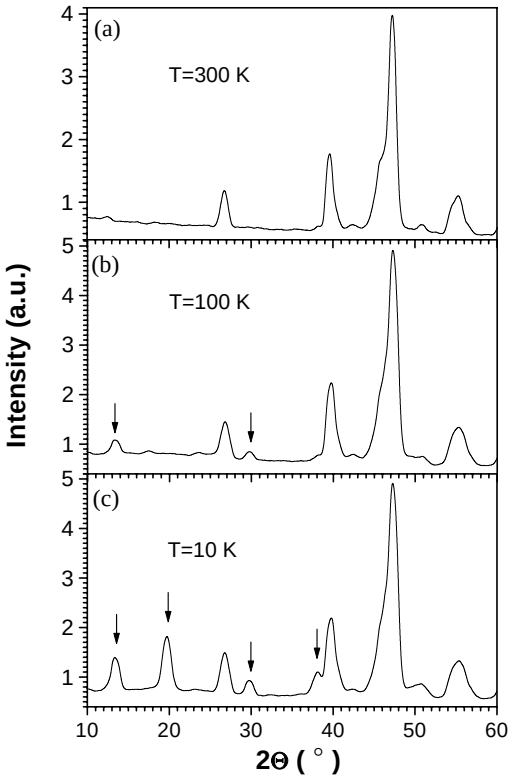

Fig. 6. Neutron diffraction patterns of $La_{0.50}Ca_{0.50}MnO_{2.50}$ sample taken at $T = 300$ K (a), 100 K (b), and 10 K (c). The arrows indicate magnetic reflexes.

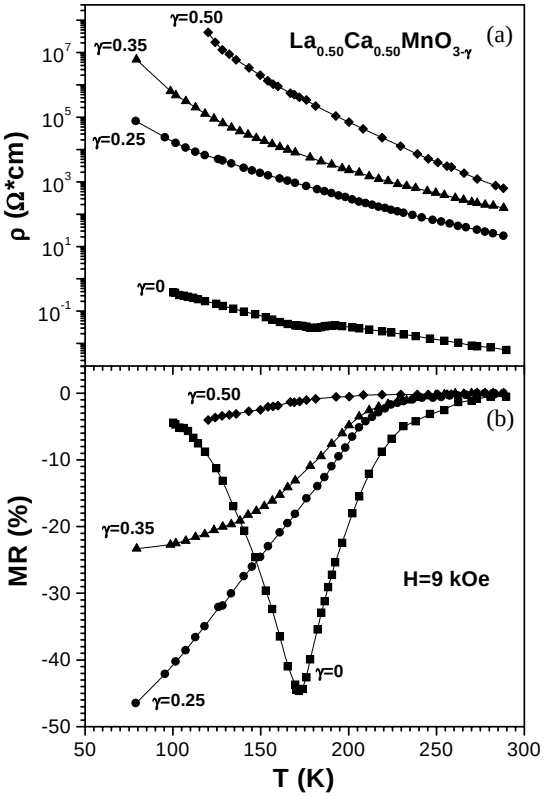

Fig. 7. The resistivity (a) and magnetoresistance (c) versus temperature curves for the $\gamma = 0$ (full square), 0.25 (full circle), 0.35 (full up-triangle) and 0.50 (full diamond) samples of the $La_{0.50}Ca_{0.50}MnO_{3-\gamma}$ reduced series.

antiferromagnetic ordering of manganese magnetic moments. The details of magnetic structure will be published shortly.

Resistivity and magnetoresistance against temperature for the $\gamma = 0$, 0.25, 0.35, 0.50 samples of the $La_{0.50}Ca_{0.50}MnO_{3-\gamma}$ series are shown in Fig. 7. There is an anomaly of resistivity for the stoichiometric sample ($\gamma = 0$) below the Curie point. Resistivity of all the reduced samples has an insulator character and continuously increases as oxygen content decreases. The peak of MR $\sim$45% was observed in the stoichiometric sample at the $T = 190$ K. This temperature is associated with antiferromagnet–ferromagnet transition [11]. For all the reduced samples MR monotonically increases with decreasing temperature. It is notable that the $\gamma = 0.25$ sample had MR value about 48%, which is comparable with those for the best samples of the $La_{1-x}Sr_xMnO_3$ system [32]. There is no metal–insulator transition as well as peak magnetoresistance for all the reduced samples. The significant MR appears below the temperature, at which magnetic ordering develops.

Summarizing our magnetization measurement results, we constructed the hypothetical magnetic phase diagrams of the $La_{0.70}Ca_{0.30}MnO_{3-\gamma}$ (Fig. 8) and $La_{0.50}Ca_{0.50}MnO_{3-\gamma}$ (Fig. 9) series.

T_{MO} for the $La_{0.70}Ca_{0.30}MnO_{3-\gamma}$ gradually decreases (Fig. 8) with increasing oxygen vacancies concentration until $\gamma = 0.06$ where it undergoes a sharp drop corresponding to destruction of long-range ferromagnetic order. The obtained experimental results may be understood in the following way. As it is known [21], both the SE Mn^{3+}–O–Mn^{4+} and Mn^{3+}–O–Mn^{3+} magnetic interactions should be positive in the orbitally disordered phase if manganese ions are surrounded by six oxygen anions. However, these interactions became antiferromagnetic in the case of 5-fold coordination of the manganese ion [33,34]. It is worth noting that DE between Mn^{3+} and Mn^{4+} ions around oxygen vacancies also should be broken. So the antiferromagnetic part of the SE interactions should enhance with increasing oxygen vacancies number, whereas double exchange gradually disappears. Small amount of oxygen vacancies $0 \leqslant \gamma \leqslant 0.06$ in $La_{0.70}Ca_{0.30}MnO_{3-\gamma}$ is sufficient only to decrease both the Curie point and the spontaneous magnetization. Further decrease of the oxygen content leads to increasing amount of Mn ions with a five-fold coordination and destroying long-range ferromagnetic order. The ferromagnetic clusters present the regions enriched with Mn^{4+} and depleted with oxygen vacancies whereas the regions with the larger oxygen vacancy content tend to order antiferromagnetically.

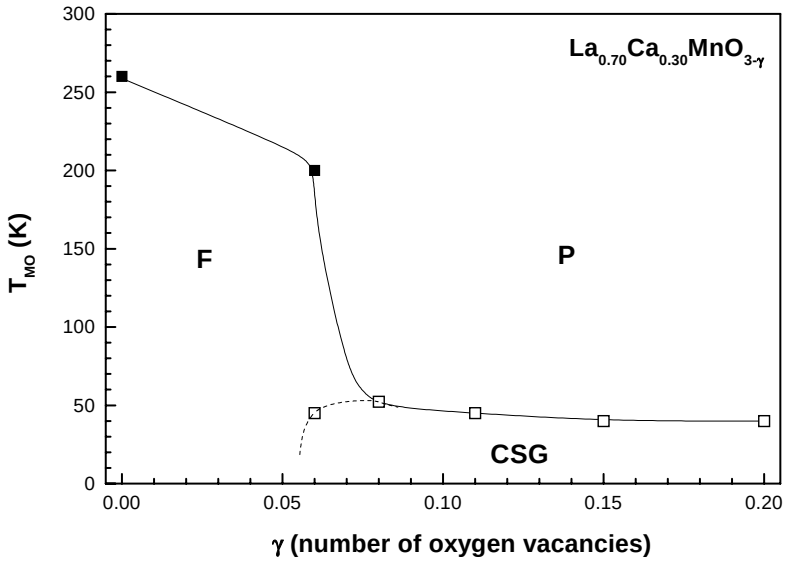

Fig. 8. The hypothetical magnetic phase diagram for the $La_{0.70}Ca_{0.30}MnO_{3-\gamma}$ reduced series. *F* denotes the ferromagnetic state, CSG the cluster spin glass one and *P* the paramagnetic.

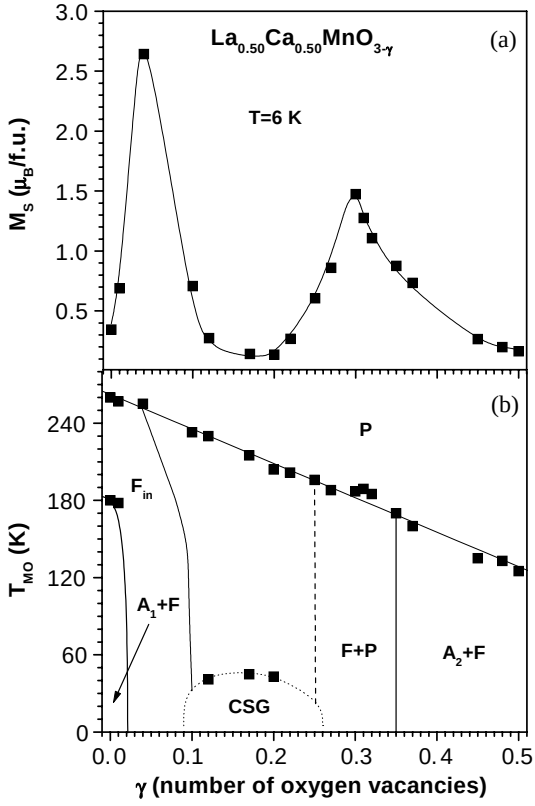

Fig. 9. The dependence of spontaneous magnetization versus a number of oxygen vacancies at 6 K (a) and the hypothetical magnetic phase diagram (b) for the $La_{0.50}Ca_{0.50}MnO_{3-\gamma}$ series. A_1 denotes the charge ordered antiferromagnet, A_2 is the charge disordered antiferromagnet F_{in} is the inhomogeneous ferromagnet, *F* is the ferromagnetic component, CSG is the cluster spin glass and *P* is the paramagnet.

Magnetic coupling between the ferromagnetic and antiferromagnetic clusters randomly distributed in space gives rise to the cluster spin glass behavior. The peak in the ZFC curve is associated with the temperature of the spin freezing of the ferromagnetic clusters into different directions as a result of the intra- and inter-cluster magnetic interactions. To explain the large magnetic susceptibility of the $\gamma = 0.20$ sample we assume that this sample contains predominantly ferromagnetic clusters. Apparently magnetic properties of this sample are strongly affected by the peculiar redistribution of the oxygen vacancies.

Compositions of the $La_{0.50}Ca_{0.50}MnO_{3-\gamma}$ series are found to undergo a number of concentration phase transitions in the ground state with decreasing oxygen content (Fig. 9). Antiferromagnetic state of the $\gamma = 0$ compound transforms into an inhomogeneous ferromagnetic one at $\gamma = 0.04$ which in turn converts into a cluster spin glass state at $\gamma \sim 0.10$. At $\gamma = 0.25$ a new type of ferromagnetic phase appears. The content of this ferromagnetic phase is the highest for the composition $\gamma = 0.30$. We suppose that at $\gamma \sim 0.50$ the samples consist of an antiferromagnetic medium and small amount the of ferromagnetic clusters taking into account neutron diffraction data (Fig. 7).

Removal of the oxygen ions challenges antiferromagnet–ferromagnet transition for $\gamma = 0.04$. It is worth recalling that the charge ordering favors antiferromagnetic properties in the manganites. It is possible that the small oxygen vacancies concentration ($0 < \gamma \leqslant 0.04$) removes the charge ordering thus leading to an increase of ferromagnetic component due to both DE and SE and at the same time slightly changes the coordination number of Mn ions. The latter process lead to enhancement of antiferromagnetic component of SE interaction.

In the concentration range $0.04 < \gamma < 0.25$, a number of Mn^{3+} in the 5-fold oxygen coordination is significant,

which gives rise to a competition between ferromagnetic and antiferromagnetic interactions. As it is well known a cluster spin glass state may result from competition between ferromagnetic and antiferromagnetic interactions. It is natural to suppose that the ferromagnetic component corresponds to oxygen-enriched microdomains whereas oxygen-poor microdomains should exhibit antiferromagnetic properties.

To explain the magnetic state of the samples for the $La_{0.50}Ca_{0.50}MnO_{3-\gamma}$ series with large oxygen vacancy concentration ($\gamma > 0.25$), we should take into account non-random distribution of the oxygen vacancies over the crystal lattice and crystal structure phase separation. We suppose the oxygen vacancies to be distributed non-uniformly in the crystal lattice of the sample at $\gamma \sim 0.25$. It is notable that the HREM study of $La_{0.50}Ca_{0.50}MnO_{2.75}$ composition taken out in [35] displays that. According to [35] the oxygen vacancies accumulate in the thick domain walls so a sample consists of planar microdomains enriched and depleted with oxygen vacancies. It is probable that both microdomains contain predominantly Mn^{3+} ions. We believe that the ferromagnetic component is connected with $La_{0.50}Ca_{0.50}MnO_{3-\lambda}$ phase which has oxygen vacancies concentration considerably above the nominal value γ. Therefore, a ferromagnetic component results from the positive Mn^{3+}(6-fold coordination)–O–Mn^{3+}(6-fold coordination) SE magnetic interactions whereas Mn^{3+}(5-fold coordination)–O–Mn^{3+}(5- or 6-fold coordination) SE ones give rise to an antiferromagnetic component.

A further removal of oxygen ions from the crystal lattice of $\gamma = 0.25$ sample leads to the formation of an $Sr_2Fe_2O_5$-type structure characterized by the microdomains with uniformly alternated [MnO_6] octahedrons and [MnO_4] tetrahedrons but no formation of brownmillerite-type one with domains containing oppositely oriented [MnO_5] square pyramids, as in $Ca_2Fe_2O_5$ [33]. Apparently, the samples in the concentration range $0.30 \leqslant \gamma \leqslant 0.50$ are mixtures of the antiferromagnetic microdomains of $Sr_2Fe_2O_5$-type structure and domains similar to the $La_{0.50}Ca_{0.50}MnO_{2.75}$-type structure. Antiferromagnetic state of the $\gamma > 0.35$ samples seems to result from both the intense negative Mn^{3+}(6-fold coordination)–O–Mn^{3+}(4-fold coordination) and the Mn^{3+}(6-fold coordination)–O–Mn^{2+}(4-fold coordination) interactions which dominate over Mn^{3+}(6-fold coordination)–O–Mn^{3+}(6-fold coordination) ferromagnetic ones.

We have already carried out the investigations of magnetic and electrical properties of $La_{1-x}Ca_xMnO_{3-x/2}$ manganites depending on the x value [24,25]. These compounds did not contain Mn^{4+} ions. It was detected that the compositions in the range $0.35 < x < 0.50$ show a strong increase in the spontaneous magnetization and critical point associated with the appearance of spontaneous magnetization. We assume that the evolution of ferromagnetic component in the compositions with calcium concentration $0.35 < x \leqslant 0.50$ may be the result of the non-random distribution of the oxygen vacancies as it was described for $\gamma = 0.25$ composition. The compound with $x = 0.50$ from [25] corresponds to that with $\gamma = 0.25$ in our case.

Our results suggest that upon reduction of the oxygen content the electrical resistivity increases dramatically. These data indicate that other factors rather than the ratio Mn^{3+}/Mn^{4+} or Mn^{3+}/Mn^{2+} play a dominant role in the determination electrical properties of $La_{1-x}Ca_xMnO_{3-\gamma}$ with less oxygen content. The resistivity of the polycrystalline samples is determined by two contributions, i.e. contributions from the intragrain regions and contribution from the intergrain regions (grain boundaries). It is well known that the reduction more likely creates oxygen vacancies at the grain boundaries because grain boundary diffusion coefficients for oxygen exceed bulk diffusion ones by more than one order of magnitude. Resistivity data of all the reduced samples are well described, assuming the appearance of the oxygen-poor microdomains on the grain surface. Oxygen ions are bridges through which the charge carriers transfer. As a result of oxygen vacancy appearance the electron transfer between grains is difficult and the resistivity is high. The extraction of oxygen from the grain boundaries leads to broadening of insulating barriers associated with intergrain boundaries so the electrical resistivity should also increase. The electrical resistivity of intragrain regions results from formation of the acceptor levels associated with $Ca^{2+} + Mn^{4+}$ pairs for stoichiometric samples. With increasing Ca^{2+} content these levels form narrow impurity band which overlaps with a wide $2p$ oxygen band as magnetic ordering occurs. We suppose that the oxygen vacancies' appearance leads to an increase of the gap between acceptor levels and $2p$-band. The factor destruction of the long-range ferromagnetic order in the $La_{0.70}Ca_{0.30}MnO_{3-\gamma}$ oxygen-deficient samples should be taken into account. This process leads again to increasing resistivity. Finally, we should note that for the strongly reduced samples oxygen vacancies tend to order thus leading to a splitting of both the $3d$ and $2p$ bands. All these processes should lead to enhancement of the resistivity.

Manganites usually show MR effect in two distinct regions. One is pronounced near the ferromagnetic (or antiferromagnetic) ordering temperature (intragrain MR), the other one is dominant at low temperature where the magnetization is substantial (intergrain MR). The physical origin of the high-temperature MR has been explained by the existence of magnetic polarons near T_C [36]. MR of the strongly reduced samples studied in this paper is negative and gradually increases

as temperature decreases. This behavior formally corresponds to the intergranular MR. The intragranular MR associated with antiferromagnet–ferromagnet and ferromagnet–paramagnet transitions is observed in the stoichiometric samples. MR of all the reduced samples seems to have two contributions: (i) decreasing gap between the impurity $3d$ levels and the wide conduction band in external magnetic field (intragrain part of MR) and (ii) tunnel character of charge carriers hopping between grains (intergrain part of MR). In a strong enough field the magnetic moments of the ferromagnetic clusters tend to align along the field direction. For cluster spin glass state this effect is more pronounced at low temperatures because magnetic order gradually enhances with temperature decrease. As a result electrons are transferred more easily between clusters and the resistivity decreases. This leads to a low-temperature intragrain MR effect.

4. Conclusions

This study has shown a large ferromagnetic component and large magnetoresistance in the $La_{1-x}Ca_xMnO_{3-\gamma}$ ($x = 0.30, 0.50$, $0 \leqslant \gamma \leqslant 0.50$)-reduced perovskite manganites in spite of the absence of Mn^{3+}–Mn^{4+} pairs. Evolution of the magnetic state in these compounds has been investigated depending on the oxygen content. Non-monotonic character of the change of the spontaneous magnetization was observed for the $La_{0.50}Ca_{0.50}MnO_{3-\gamma}$ samples versus γ. A large magnetoresistance of the strongly reduced samples has been observed below temperature where the spontaneous magnetization develops. Magnetic phase diagrams for the $La_{0.70}Ca_{0.30}MnO_{3-\gamma}$ and $La_{0.50}Ca_{0.50}MnO_{3-\gamma}$ series have been constructed and discussed. The Mn^{3+}–O–Mn^{3+} interactions were assumed to be isotropic and positive in the orbitally disordered state. Ferromagnetic component seemed to result from the competition between positive SE Mn^{3+}(6-fold coordination)–O–Mn^{3+}(6-fold coordination), as well as Mn^{3+}(6-fold coordination)–O–Mn^{4+}(6-fold coordination) and negative SE Mn^{3+}(6-fold coordination)–O–Mn^{3+}(5-fold coordination) as well as Mn^{3+}(6-fold coordination)–O–Mn^{2+}(5-fold coordination) interactions. To explain the obtained experimental results the oxygen vacancies were supposed to be disordered in the $La_{0.70}Ca_{0.30}MnO_{3-\gamma}$ ($\gamma \leqslant 0.15$) series of compounds whereas for $\gamma = 0.20$ peculiar oxygen redistribution seemed to exist. For the $La_{0.50}Ca_{0.50}MnO_{3-\gamma}$ the oxygen vacancies were disordered at $\gamma \leqslant 0.20$, whereas in the vicinity $\gamma \sim 0.25$, there is a trend to vacancies ordering in microdomains having a form of thin planes. For compositions with oxygen content close to $\gamma = 0.50$, the oxygen vacancies ordering corresponds to the $Sr_2Fe_2O_5$ structure. The investigations have contributed in understanding the magnetic interactions in the selected compounds of manganites with different values of average valence of the manganese ions.

Acknowledgments

This work was supported by Belarus Fund of Fundamental Research (F02M-069), the European Community-Access to Research Infrastructure action of Improving Human Potential Program (contract HPRI-CT-1999-00020), DFG (Germany), and Polish Committee for Scientific research (KBN Grant 5 PO3B 016 20).

References

[1] S. Jin, et al., Phys. Rev. Lett. 264 (1994) 413.
[2] H.W. Hwang, S.-W. Cheong, et al., Phys. Rev. Lett. 75 (1995) 914.
[3] G. Matsumoto, J. Phys. Soc. Jpn. 29 (1970) 606.
[4] G. Matsumoto, J. Phys. Soc. Jpn. 29 (1970) 615.
[5] K. Kubo, J. Phys. Soc. Jpn. 33 (1972) 21.
[6] K. Kubo, J. Phys. Soc. Jpn. 33 (1972) 929.
[7] P. Shiffer, A.P. Ramirez, W. Bao, et al., Phys. Rev. Lett. 75 (1995) 3336.
[8] A. Urushibara, Y. Moritomo, T. Arima, et al., Phys. Rev. B 51 (1995) 14103.
[9] G.H. Jonker, J.H. Van Santen, Physica (Utrecht) 16 (1950) 337.
[10] S. Jin, T.H. Tiefel, M. McCormack, et al., Science 264 (1994) 413.
[11] J.W. Lynn, R.W. Erwin, J.A. Borchers, Q. Huang, et al., Phys. Rev. Lett. 76 (1996) 4046.
[12] F. Rivadulla, M. Freita-Alvite, M.A. López-Quintela, et al., J. Appl. Phys. 91 (2002) 785.
[13] P. Levy, F. Parisi, G. Polla, et al., Phys. Rev. B 62 (2000) 6437.
[14] J.B. Goodenough, Phys. Rev. 100 (1955) 564.
[15] C.H. Chen, S.-W. Cheong, Phys. Rev. Lett. 76 (1996) 4042.
[16] C.N. Rao, A. Arulraj, P.N. Santosh, A.K. Cheetham, Chem. Mater. 10 (1998) 2714.
[17] C. Zener, Phys. Rev. 82 (1951) 403.
[18] P.-G. De Gennes, Phys. Rev. 118 (1960) 141.
[19] I.O. Troyanchuk, D.D. Khalyavin, E.F. Shapovalova, et al., Phys. Rev. B 58 (1998) 2422.
[20] I.O. Troyanchuk, S.V. Trukhanov, H. Szymczak, et al., J. Phys.: Condens. Matter 12 (2000) L155.
[21] J.B. Goodenough, A. Wold, R.J. Arnott, N. Menyuk, Phys. Rev. 124 (1961) 373.
[22] S.V. Trukhanov, I.O. Troyanchuk, F.P. Korshunov, et al., Low Temp. Phys. 27 (2001) 247.
[23] V. Caignaert, F. Millange, B. Domenges, B. Raveau, Chem. Mater. 11 (1999) 930.
[24] I.O. Troyanchuk, D.D. Khalyavin, S.V. Trukhanov, et al., JETP Lett. 70 (1999) 590.
[25] I.O. Troyanchuk, S.V. Trukhanov, H. Szymczak, J. Przewoznik, K. Bärner, JETP 120 (2001) 183.
[26] S.V. Trukhanov, I.O. Troyanchuk, I.M. Fita, H. Szymczak, K. Bärner, J.Magn Magn. Mater. 237 (2001) 276.
[27] Von M. Harder, Hk. Muller-Buschbaum, Z. Anorg. Allg. Chem. 464 (1980) 169.

[28] J.M. Gonzalez-Calbet, M. Vallet-Regi, et al., Mater. Res. Bull. 18 (1983) 285.
[29] J. Töpfer, J.B. Goodenough, J. Solid State Chem. 130 (1997) 117.
[30] K. Nakamura, K. Ogawa, J. Solid State Chem. 163 (2002) 65.
[31] R.D. Shannon, Acta Crystallogr. A 32 (1976) 751.
[32] L. Balcells, A.E. Carrillo, B. Martinez, J. Fontcuberta, Appl. Phys. Lett. 74 (1999) 4014.
[33] K.R. Poeppelmeier, M.E. Leonowicz, J.M. Longo, J. Solid State Chem. 44 (1982) 89.
[34] K.R. Poeppelmeier, M.E. Leonowicz, J.C. Scanlon, J.M. Longo, W.B. Yelon, J. Solid State Chem. 45 (1982) 71.
[35] J.M. Gonzalez-Calbet, E. Herrero, N. Rangavittal, et al., J. Solid State Chem. 148 (1999) 158.
[36] H.L. Ju, C. Kwon, Qi Li, R.L.Greene, T. Venkatesan, Appl. Phys. Lett. 65 (1994) 2108.